Int. J. Solids Structures Vol. 23, No. 6, pp. 733–750, 1987
Printed in Great Britain.

0020-7683/87 $3.00 + .00

CONSTITUTIVE MODEL WITH STRAIN SOFTENING

G. FRANTZISKONIS and C. S. DESAI
Department of Civil Engineering and Engineering Mechanics, University of Arizona, Tucson, AZ 85721, U.S.A.

(*Received* 20 *June* 1985; *in revised form* 10 *July* 1986)

Abstract—The aim of this paper is to propose a simple yet realistic model for the mechanical behavior of geologic materials such as concrete and rock. The effect of structural changes in such materials is addressed and incorporated in the theory through a tensor form of a damage variable. It is shown that formation of damage is responsible for the softening in strength observed in experiments, for the degradation of the elastic shear modulus, and for induced anisotropy. A generalized plasticity model is incorporated for the so-called topical or continuum part of the behavior, whereas the damage part is represented by the so-called stress-relieved behavior. The parameters required to define the model are identified and determined from multiaxial testing of a concrete. The predictions are compared with observed behavior for a number of stress paths. The model shows very good agreement with the observed response.

1. INTRODUCTION

A basic hypothesis in constitutive modelling is the concept of a continuum in which stress, strain, density, etc., are assumed to be defined at every point in the continuum. Under this assumption, material properties can be determined from tests on finite sized specimens undergoing homogeneous stress and strain. As the stress and strain deviate significantly from homogeneity, the observed behavior may no longer represent (continuum) material properties. Due to difficulties in identifying the influence of such nonhomogeneities, it is often ignored, and the observed load–deformation relations of finite sized specimens are "translated" as stress–strain relations. However, influence of the nonhomogeneity can be very important in interpreting certain types of behavior such as softening in geologic materials. Softening can be described as decrease in strength during progressive straining after a peak strength value has been reached. Various limitations arise when strain softening is treated as a (continuum) material property[1–5], with respect to solutions of boundary value and initial value problems. Also, there is experimental evidence indicating that strain softening is not a material property of concrete, rock or soil treated as continua, but rather the performance of a structure (e.g. a finite sized specimen) in which the individual components such as microcracks, joints and interfaces result in an overall loss of strength with progressive straining[1, 2, 6–10].

Comprehensive reviews of models for strain softening and for the subject of microcracking and fracture are not attempted herein; such reviews are given in Refs [2, 11]. However, references are made to those works that are directly relevant to this study. Clearly development of a model that considers in detail all the structural changes (e.g. microcrack propagation) in concrete and rock-like materials is not easy. However, it is possible to model the average influence of the structural changes, and such an approach is followed in this paper. It is recognized that the total deformation in such materials is attributed to elastic deformation, plastic flow, and to formation of damage. The damage can be caused mainly due to pre-existing microfracture, and microfracture planes that initiate and subsequently grow.

In the model proposed herein, behavior of an element (specimen) is decomposed in two parts. The first part with volume V_t, representing topical (continuum) behavior, which is *non-softening* and obeys an elastoplastic constitutive law. In the second part, which refers to the damaged or fractured part with volume V_0, the behavior is such that its stiffness is assumed to be zero. At every finite material element the total volume is V; therefore, $V = V_t + V_0$. Details on this decomposition are given subsequently. It is shown that the proposed model is relatively simple, and that it can capture the essential feature of concrete

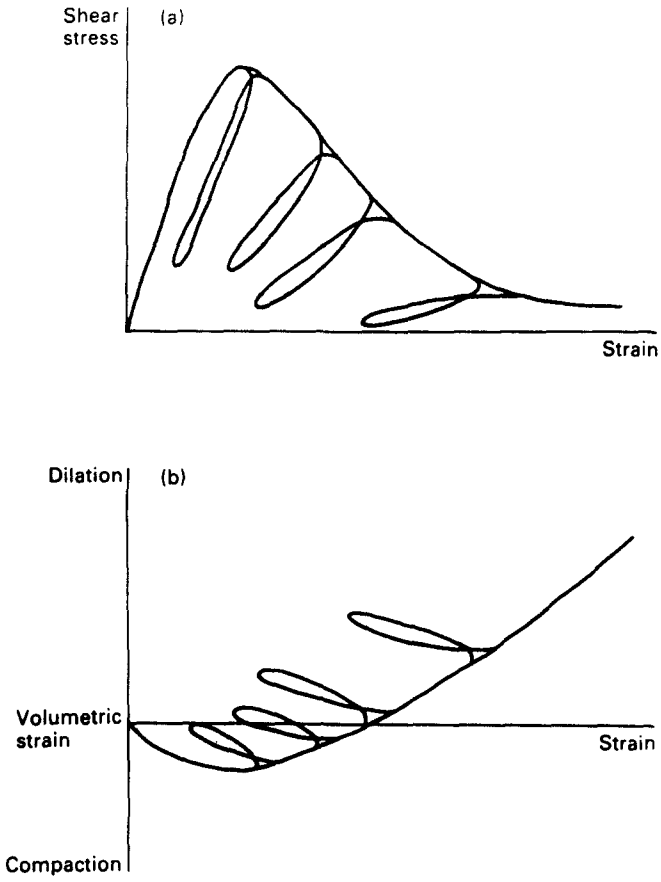

Fig. 1. Schematic of experimental stress–strain response: (a) stress–strain behavior; (b) volumetric behavior.

and rock behavior under general triaxial compressive loading[12] such as: (1) softening under monotonic shear loading, (2) shear stiffness degradation under progressive loading, and (3) dilatant behavior under monotonic shear loading. These features are shown schematically in Fig. 1 where stress and strain denote average values as measured from the experiment and not the actual stress and strain at a local level.

The proposed model can be seen as an extension of the uniaxial model proposed by Kachanov[13] and Rabotnov[14]. However, the distinguishing feature is that damage in the proposed model is represented through a second-order tensor, which has a physical meaning. In order for such a multiaxial model to be rational, it should be able to predict damage induced anisotropy observed in brittle materials because microcracks follow preferred orientations. Here, it is appropriate to quote Drucker[15] that "an almost limitless field of useful and difficult research lies ahead in the extension of the damage approach pioneered by Kachanov and Rabotnov".

Strain level at peak strength of concrete or rock is of the order of 0.3% and at the residual strength of the order of 3.0%. These strain levels are considered as small, and thus small deformation theory is employed in the present paper, recognizing that the theory can be extended to large deformations with appropriate modification of the static and kinematic variables.

2. REVIEW

Few theoretical models have been proposed in the literature that can capture the essential features of the behavior of concrete and rock, as described previously. The models based on characterization of damage will be briefly discussed subsequently. Mathematical

characterization of damage as well as physical interpretation of damage parameters differ, depending on the material, availability and interpretation of test results, and the assumptions made.

Desai[16] proposed a model for strain softening behavior for overconsolidated soils (and interfaces) in which the material response is decomposed in two (or more) components: one due to a basic, normally consolidated part and the other due to an overconsolidation that contributes to strain softening. The resulting model modifies the initial constitutive matrix through a function that allows for strain softening. The moduli are expressed in terms of various physical factors such as peak and residual stresses and strains, areas under the component curves and initial moduli. The progress of softening is defined in terms of peak and residual quantities; a similar approach is used for description of the damage evolution proposed in this study.

In the approach followed in Refs [13, 14], under uniaxial conditions, a scalar is defined such that it represents a measure of the voids in a cross-section of a specimen subjected to uniaxial stress. The scalar is defined as the quotient between intact cross-sectional area and total macroscopic cross-sectional area. The theory was implemented for prediction of the creep behavior of metals. Problems of creep damage have been investigated by many authors[17, 18]. In Ref. [18], the finite element method was used to show how stresses, within a tension plate containing a circular hole, redistribute due to creep deformation. Loland[19] proposed a damage model for the behavior of concrete under uniaxial tension. The model assumes that defects are initially present and start propagating under loading. Tensile strains are considered to cause damage accumulation. A similar model was proposed by Mazars[20].

The aspect of both degradation of strength and stiffness was adopted in a theory of progressively fracturing solids[21, 22]. Underlying the progressively fracturing theory is an energy dissipation function which takes essentially the shape of the energy requirement curve for stable crack propagation. A plastic fracturing variant of the progressively fracturing solid was proposed in Ref. [23]. The theory combines the plastic stress decrements with the fracturing stress decrements to account for strain softening and degradation of elastic moduli due to microcracking. The concept of a material-specific element of irreducible size is used in Ref. [24] where a model based on a vector damage function[25] is developed. In Ref. [26], the method of slices is employed to interpret the fact that softening in the triaxial test is due mainly to geometric effects.

3. EFFECT OF STRUCTURAL CHANGES

Microcrack initiation, microcrack propagation and joining of microcracks are the major structural changes in concrete and rock. The laws that govern the above structural changes are not fully understood, but it is an experimental fact that they affect considerably the behavior of these materials. Following Ref. [12], we describe in a qualitative manner the effect of crack extension and crack joining. In the initial loading stage, fracture sites may be considered uniformly distributed. Qualitatively, the effect of an isolated fracture site is that a stress-relieved zone exists around it and a potential crack extension site at its edges, as shown schematically in Fig. 2. Under continuous loading, stress-relieved zones increase (Fig. 2). Upon further increase in overall stress, isolated cracks join and finally continuous macrocracks are developed. At this stage, the volume of the stress-relieved zones is close to the total volume. In order to give a physical insight into the damage characterization defined subsequently, we note the volume of the stress-relieved zones as V_0 and the total volume as V. Obviously, V_0 increases during loading, and at every stage $V_t = V - V_0$ where V_t is defined as the topical fraction of the total volume; the latter part of the body is assumed to obey an elastic–plastic constitutive relation.

4. BASIC HYPOTHESIS IN CHARACTERIZATION OF STRUCTURAL CHANGES

In the Introduction, it was mentioned that in the proposed model the average material response is decomposed in two parts. Here, we describe this concept in more detail. It is assumed that topical material elements of volume V_t obey an elastoplastic constitutive

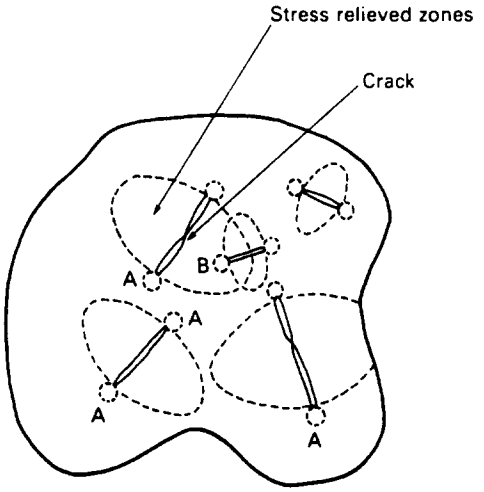

Fig. 2. Schematic of stress relieved zone and crack propagation sites (after Van Mier[12]): A, potential crack extension site; B, unlikely site for crack growth.

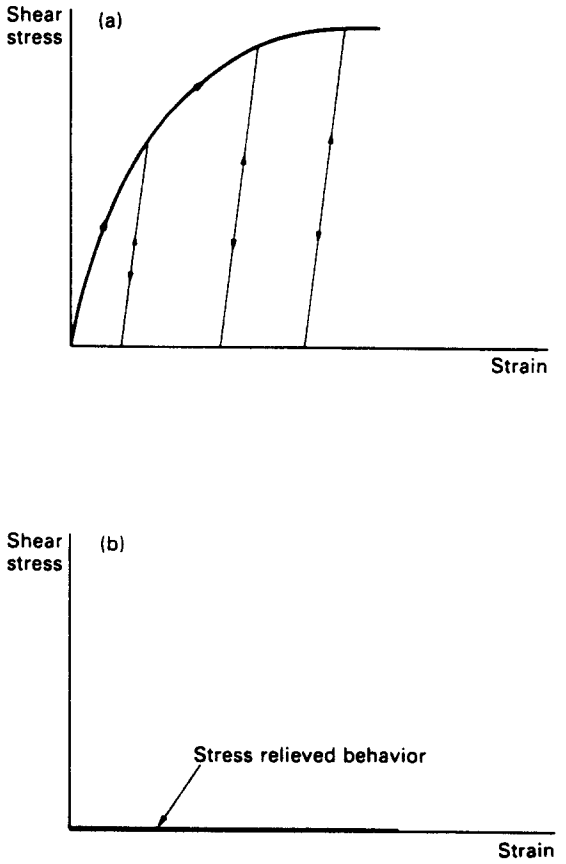

Fig. 3. Components of stress–strain response: (a) elastic–plastic stress–strain curve; (b) stress relieved stress–strain curve.

relation (Fig. 3(a)) and the stress-relieved material elements of volume V_0, a law as depicted in Fig. 3(b), as rigid, perfectly plastic with zero yield strength.

Let $r = V_0/V$ $(0 \leqslant r \leqslant 1)$ with the interpretation that before any load is applied, $r = 0$ and if under monotonic loading the residual stress level is reached, r reaches an ultimate value, r_u, which can tend to 1. In this model, r is treated as a continuum field variable over the entire body instead of at isolated parts of the body. Then for compatibility at the

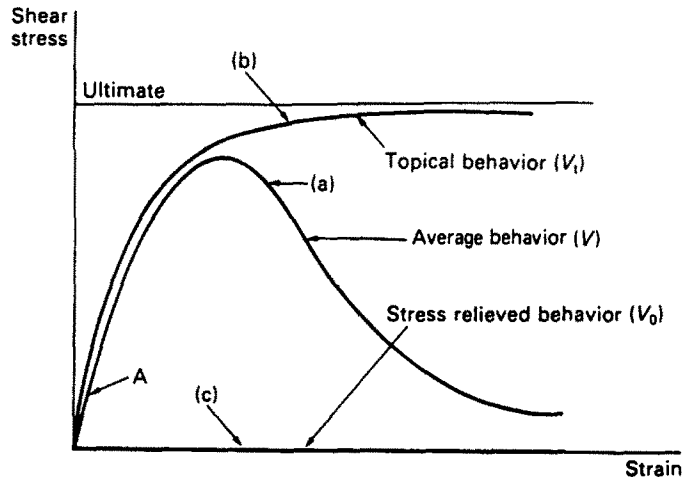

Fig. 4. Concept of decomposition of material behavior.

continuum level, strains in V_0 are considered equal to strains in V_t. Consequence of the decomposition is depicted in Fig. 4 where behavior corresponding to volumes V, V_t and V_0 are schematically shown. The topical behavior for V_t, curve (b) in Fig. 4, plus the stress-relieved behavior for V_0, curve (c), result in the average behavior for the total volume V, curve (a). For monotonic loading, V_0 continuously increases and V_t continuously decreases. By average behavior, we mean the gross behavior; for example, stress–strain results obtained from a (uniaxial) compression test, and it is typically represented by curve (a) in Fig. 4. We now explain the assumptions and approximations involved in the proposed model.

Let the topical stress tensor be denoted as σ'_{ij} and the average stress tensor as σ_{ij}. From the above decomposition, it is concluded that the average stress is related to the topical stress and the values of volumes V_0 and V_t. The deviatoric stress at the stress-relieved volume is not included in such a relation since it is zero (Fig. 4). In order to establish this relation, use of experimental observations is made [12]. For hydrostatic compression loading, microcracks tend to close and thus no significant damage is recorded. This can imply that damage is caused from the deviatoric component; thus, the topical and average stress lie on the same deviatoric plane, as shown in Fig. 5(a), where it is assumed that the hydrostatic stresses in the topical and damaged parts are equal. Now we consider a stress path such that, e.g. two of the principal stresses of σ_{ij} are equal; that is, $\sigma_2 = \sigma_3$. Then the σ_{ij} tensor is positioned as shown in Fig. 5(b). In this stress path, cylindrical symmetry exists and if the material is assumed as initially isotropic, this symmetry is maintained through the above stress path. Then this symmetry must be reflected in the topical stress tensor; thus $\sigma'_2 = \sigma'_3$. Then the topical stress tensor σ'_{ij} is positioned as shown in Fig. 5(b). The above considerations lead to the assumption that σ_{ij} and σ'_{ij} lie on a line perpendicular to the hydrostatic axis, as shown in Fig. 5(c). When there is no damage induced, $r = 0$ and $\sigma_{ij} = \sigma'_{ij}$ or (AC) = (BC) in Fig. 5(c). When the residual stress level is reached, damage is maximum and $r = r_u$. This implies that distance (AB) in Fig. 5(c) is small, representing the residual stress level. Based on these considerations, it is proposed that the distances (BC) and (AC) are connected through (AB) = (AC) $(1 - r)$, or

$$\sqrt{J_{2D}} = \sqrt{J'_{2D}}(1 - r) \tag{1}$$

where $\sqrt{J_{2D}}$ is the stress intensity of σ_{ij} defined as $\sqrt{J_{2D}} = (\frac{1}{2}S_{ij}S_{ij})^{1/2}$ and S_{ij} is the deviatoric part of σ_{ij} such that $\sigma_{ij} = S_{ij} + \frac{1}{3}\sigma_{kk}\delta_{ij}$. Here summation notation is implied and δ_{ij} denotes the Kronecker delta. A similar definition holds for $\sqrt{J'_{2D}}$. Through eqn (1)

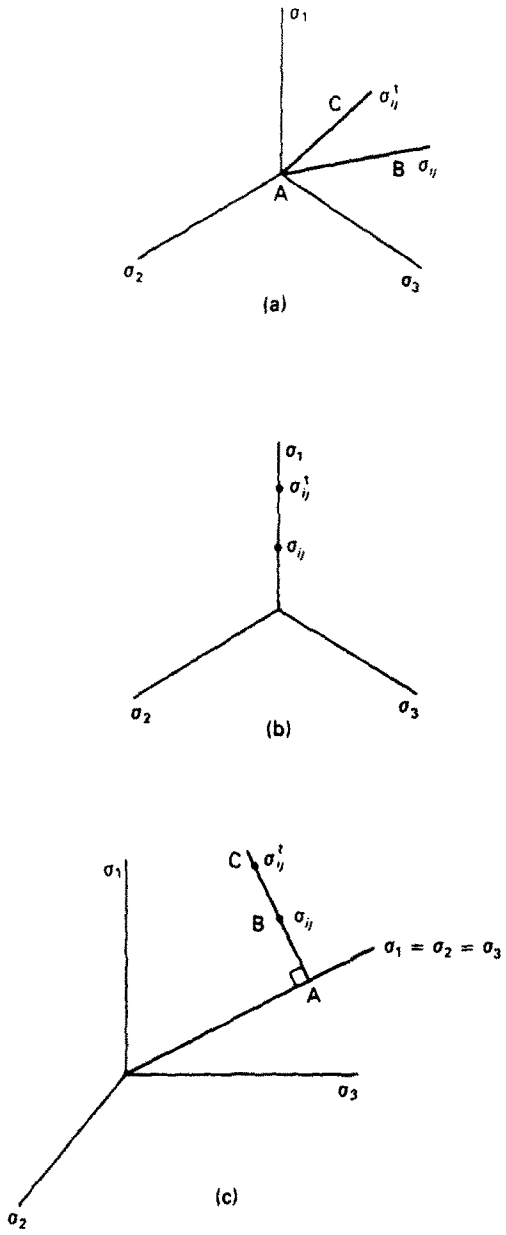

Fig. 5. Relative position of σ^i_{ij} and σ_{ij}: (a) in the deviatoric plane ($\sigma^i_{kk} = \sigma^m_{kk}$); (b) in the deviatoric plane $\sigma_1 = \sigma_3$; (c) in principal stress space.

and the fact that σ_{ij} and σ^i_{ij} lie on a line perpendicular to the hydrostatic axis, we obtain the tensorial equivalent of eqn (1)

$$\sigma_{ij} = (1 - r)\sigma^i_{ij} + \frac{r}{3}\sigma^i_{kk}\delta_{ij}. \tag{2}$$

It is noteworthy that the two fractions described above can be considered as a mixture of the topical (intact) and the damaged part. Then the theory of mixtures or interacting components may be employed. In Ref. [27] it is shown that eqn (2) can be derived from the theory of mixtures and the assumptions discussed above that the shear stress in the damaged fraction is zero ($S^0_{ij} = 0$) and that the hydrostatic stress in the two fractions are equal ($\sigma^i_{kk} = \sigma^0_{kk}$).

Relation (2) has the following desirable properties: (1) for $r = 0$, $\sigma_{ij} = \sigma^i_{ij}$, (2) when

specialized to hydrostatic compression, it yields $\sigma_{kk} = \sigma'_{kk}$ and (3) for $r = r_u \cong 1$, $S_{ij} = (1 - r_u)S'_{ij}$, and this implies that shear stresses are significantly reduced as happens at the residual stress level. It is shown subsequently that through relation (2) essential features of concrete or rock behavior can be modelled satisfactorily.

For tensile conditions, relation (2) is not valid since, e.g. it would predict no damage progression for a hydrostatic tension stress path. It is our interpretation of experimental results that criteria for damage initiation and progression under tensile conditions are different than criteria for compressive states of stress. Thus for tensile conditions, a relation between σ_{ij}, σ'_{ij} and r can be assumed but such a relation would be different from eqn (2).

As already mentioned, material behavior is decomposed in two parts. The topical part of the decomposed behavior obeys an elastoplastic law given by

$$d\sigma'_{ij} = C^{ep}_{ijkl}\, d\varepsilon_{kl} \tag{3}$$

and for elastic unloading

$$d\sigma'_{ij} = C^{e}_{ijkl}\, d\varepsilon_{kl}. \tag{4}$$

Here, $d\sigma'_{ij}$ denote increments of stress tensor σ'_{ij}, $d\varepsilon_{kl}$ denote increments of the strain tensor, C^{ep}_{ijkl} is the elastoplastic constitutive tensor involving a yield surface and hardening rule described subsequently, C^{e}_{ijkl} is the elasticity tensor; elasticity in the present case is assumed linear and isotropic. The usual loading–unloading elastic–plastic criteria hold here[28].

5. DEGRADATION OF ELASTIC SHEAR MODULUS

Consider a loading stress path such that plastic deformation as well as damage have been induced. Then $0 < r < r_u$. It is assumed here that no damage is induced under unloading. Then if unloading follows, we have from eqn (2), with r = constant

$$d\sigma_{ij} = (1 - r)\, d\sigma'_{ij} + \frac{r}{3} d\sigma'_{kk}\, \delta_{ij} \tag{5}$$

and since unloading is elastic, eqn (4) holds. From eqns (4) and (5)

$$d\sigma_{ij} = (1 - r)[2\mu\, d\varepsilon_{ij} + \lambda\, d\varepsilon_{kk}\, \delta_{ij}] + \frac{r}{3}(2\mu + 3\lambda)\, d\varepsilon_{kk}\, \delta_{ij} \tag{6}$$

where λ, μ are Lame's constants.

Specializing eqn (6), we have

$$d\sigma_{12} = 2\mu(1 - r)\, d\varepsilon_{12}. \tag{7}$$

Thus, unloading shear modulus depends on r where r = constant for unloading, and since r increases with loading, shear modulus degrades as shown schematically in Fig. 6. This fact is well documented experimentally[12, 29–31]. Theoretically, this is treated as a result of brittle–plastic behavior[23] or as an elastic–plastic coupling problem[32–35]. It is also noted that when eqn (6) is specialized for hydrostatic compression, we have

$$d\sigma_{kk} = (2\mu + 3\lambda)\, d\varepsilon_{kk} \tag{8}$$

and thus the bulk modulus is independent of r (constant).

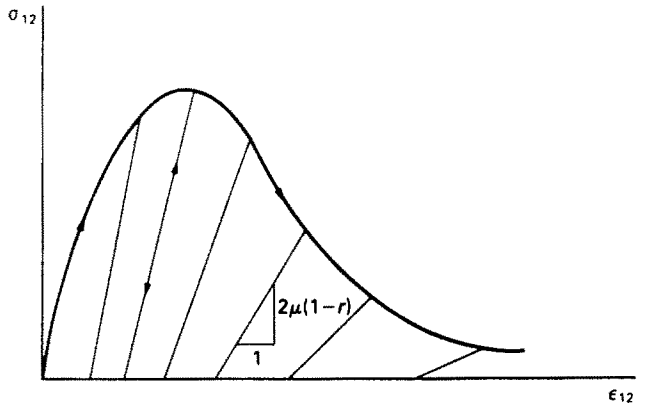

Fig. 6. Degradation of elastic shear modulus.

6. INDUCED ANISOTROPY

Another important aspect is that of induced anisotropy. During deviatoric loading, since r is not constant, from eqn (2), we have for loading

$$d\sigma_{ij} = \frac{\partial \sigma_{ij}}{\partial \sigma'_{kl}} d\sigma'_{kl} + \frac{\partial \sigma_{ij}}{\partial r} dr. \tag{9}$$

Also, from eqn (2)

$$\frac{\partial \sigma_{ij}}{\partial \sigma'_{kl}} = (1 - r)\delta_{ik}\delta_{jl} + \frac{r}{3}\delta_{ij}\delta_{pk}\delta_{pl}. \tag{10}$$

From eqn (10), we have

$$\frac{\partial \sigma_{ij}}{\partial \sigma'_{kl}} d\sigma'_{kl} = (1 - r)\, d\sigma'_{ij} + \frac{r}{3} d\sigma'_{pp}\delta_{ij}. \tag{11}$$

Also, from eqn (2)

$$\frac{\partial \sigma_{ij}}{\partial r} = -\sigma'_{ij} + \frac{1}{3}\sigma'_{pp}\delta_{ij} = -S'_{ij}. \tag{12}$$

From eqns (3), (9), (11) and (12), we obtain

$$d\sigma_{ij} = (1 - r)C^{e\text{-}p}_{ijkl}\, d\varepsilon_{kl} + \frac{r}{3}\delta_{ij}C^{e\text{-}p}_{ppkl}\, d\varepsilon_{kl} - dr\, S'_{ij}. \tag{13}$$

Relation (13) is the incremental constitutive relation relating $d\sigma_{ij}$ and $d\varepsilon_{ij}$.

In the absence of damage ($r = dr = 0$), eqn (13) yields elastoplastic hardening stress–strain response. The presence of damage modifies the involved elastoplasticity such that eqn (13) holds. Since S'_{ij} is a deviatoric tensor and since for loading $dr \neq 0$, the term $dr\, S'_{ij}$ in eqn (13) provides a measure of mechanical, damage induced anisotropy to the overall stress–strain response. Also, although r and dr are scalars, a second-order tensor, $dr\, S'_{ij}$, is involved in the stress–strain response. The overall effect of this tensorial internal variable is such that strain softening and damage induced anisotropy can be attributed to it.

7. ELASTOPLASTICITY RELATIONS

In this section, we give details of the derivation of the elastic–plastic relation for the topical part. A general hierarchical procedure for developing elastic–plastic models for isotropic and anisotropic hardening, nonassociative and strain softening responses and applications for soils, rocks and concrete are described in Refs [36–42]. This approach is used herein to describe the topical part with basic isotropic hardening and associative model, δ_0; here δ_0 denotes zero deviation from normality. Hence, the model proposed herein with the damage parameter r is termed as δ_{0+r}[41]. It is assumed that the associative flow rule holds, and the yield function is given by[41, 42]

$$F = J'_{2D} - \left\{\frac{-\alpha}{\alpha_0^{n-2}}(\bar{J}'_1)^n + \gamma(\bar{J}'_1)^2\right\}(1 - \beta S_r)^{-1/2} \tag{14}$$

where $\bar{J}'_1 = J'_1 - b$, and b is a material constant representing the distance from the stress origin to the intersection of the surface with the tensile hydrostatic axis, $J'_1 = \sigma'_{kk}$ is the first invariant of the topical stress tensor, $S_r = (J'_{3D})^{1/3}/(J'_{2D})^{1/2}$ is a stress ratio, J'_{3D} is the third invariant of the deviatoric part of σ'_{ij} defined as $J'_{3D} = \frac{1}{3}S'_{ij}S'_{jk}S'_{ki}$, β, γ, n are assumed to be material constants, and α is the growth function dependent on ξ in the manner

$$\alpha = \frac{\alpha_1}{\xi^{\eta_1}} \tag{15}$$

where $d\xi = (d\varepsilon^p_{ij}\, d\varepsilon^p_{ij})^{1/2}$, superscript p indicating plastic, and α_1, η_1 are the hardening constants; $\alpha_0 = 1$ unit of stress. The yield function in eqn (14) is isotropic since it is expressed in terms of the stress invariants. It is a closed three-dimensional surface, and intersects the hydrostatic axis at 90°; plots of eqn (15) in $\bar{J}'_1 - \sqrt{J'_{2D}}$ space and in the octahedral space are shown in Fig. 7 for a concrete described subsequently. The shape of F in Fig. 7(b) is triangular with rounded corners. For simulating the realistic behavior of concrete, the shape should approach to circular as J_1 increases. This has been achieved by expressing parameter β as a function of J_1[43].

In order to derive the C^{ep}_{ijkl} tensor, the usual relations of elastic–plastic theory are used[28]

$$d\varepsilon_{ij} = d\varepsilon^e_{ij} + d\varepsilon^p_{ij} \tag{16}$$

that is, strain increments $d\varepsilon_{ij}$ are decomposed into elastic strain increments $d\varepsilon^e_{ij}$ and plastic strain increments $d\varepsilon^p_{ij}$ and are given by

$$d\varepsilon^p_{ij} = k\lambda\frac{\partial F}{\partial \sigma'_{ij}} \tag{17}$$

known as the flow rule

$$k = \begin{cases} 1 & \text{if } F = 0 \text{ and } \dfrac{\partial F}{\partial \sigma'_{kl}} d\sigma'_{kl} > 0 \\ 0 & \text{otherwise} \end{cases}. \tag{18}$$

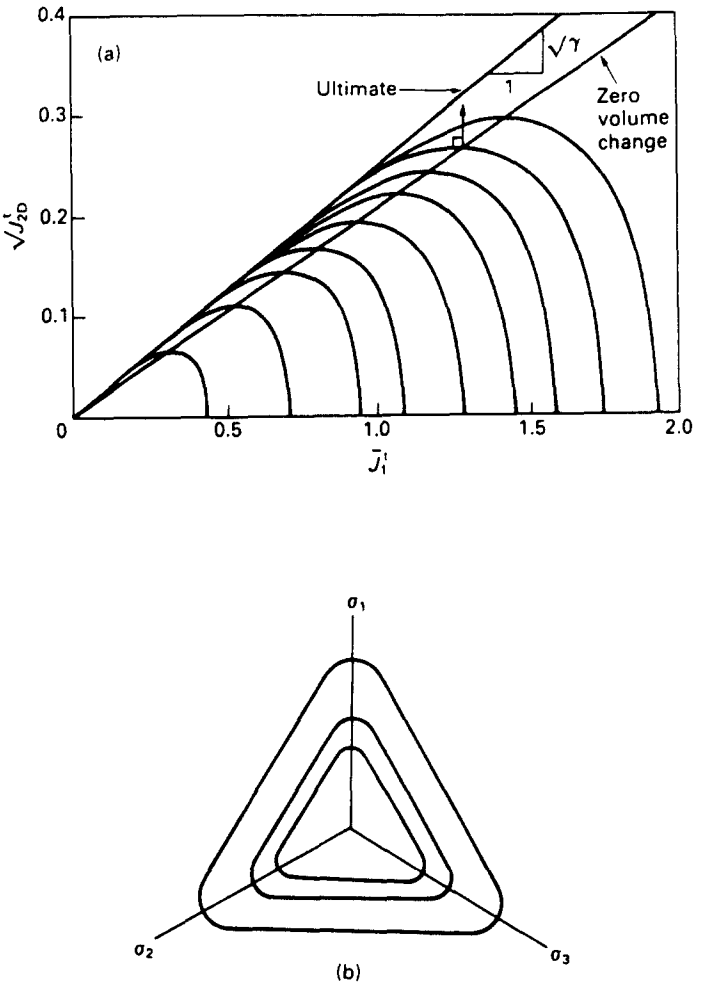

Fig. 7. Plots of the yield function F in various stress spaces: (a) J'_1–$\sqrt{J'_{2D}}$ plane; (b) octahedral plane.

For a hardening material $\lambda \geqslant 0$ and in the present theory the topical behavior is hardening (non-softening) and thus $\lambda \geqslant 0$. Relations (15)–(18) together with the consistency condition $dF = 0$ and the elasticity relation $d\sigma'_{ij} = C'_{ijkl}\, d\varepsilon^e_{kl}$ yield

$$C^{e\text{-}p}_{ijkl} = \left[C^e_{ijkl} - \frac{C^e_{ijpq}\dfrac{\partial F}{\partial \sigma_{pq}}\dfrac{\partial F}{\partial \sigma_{mn}} C^e_{mnkl}}{\dfrac{\partial F}{\partial \sigma_{uv}} C^e_{uvrs}\dfrac{\partial F}{\partial \sigma_{rs}} - \dfrac{\partial F}{\partial \xi}\left(\dfrac{\partial F}{\partial \sigma_{kl}}\dfrac{\partial F}{\partial \sigma_{kl}}\right)^{1/2}} \right] . \tag{19}$$

8. EVOLUTION OF DAMAGE AND DETERMINATION OF PARAMETERS

In the previous description, a variable, r, was introduced. Now, we define an evolution law for r in order that the formulation is complete. We exclude the possibility of r being dependent on stress since r would be affected by unloading and this contradicts our initial assumption and experimental fact of no damage accumulation during unloading. For the same reason, elastic strains are excluded. Then, generally we can write $r = f(\varepsilon^p_{ij})$ and since no damage is accumulated for (initial) hydrostatic compression, volumetric plastic strains

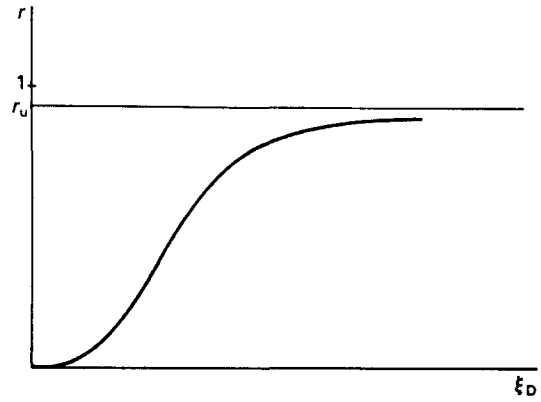

Fig. 8. Damage evolution law.

are excluded and thus we write $r = f(e^p_{ij})$ where e^p_{ij} denotes the deviator part of ε^p_{ij} such that $e^p_{ij} = \varepsilon^p_{ij} - \frac{1}{3}\varepsilon^p_{kk}\delta_{ij}$. In order to include effects of history of deviatoric plastic strains, we write

$$r = f(\xi_D) \tag{20}$$

where

$$d\xi_D = (de^p_{ij}\, de^p_{ij})^{1/2}. \tag{21}$$

In accordance with experiments[12], for low stress levels no significant damage is induced. Thus, for continuity of the stress–strain curve at point A in Fig. 4, the slope of the r vs ξ_D curve at the origin should be zero (Fig. 8). Also, when the residual stress level is reached, $r = r_u$ where $0 < r_u \leqslant 1$. Here we propose that r_u is reached asymptotically (Fig. 8). We note here that the shape of the damage evolution curve in Fig. 8 is similar in shape to the energy dissipation curve in Ref. [30].

The following function is proposed to define r:

$$r = r_u - r_u \exp(-\kappa \xi_D^R) \tag{22}$$

where r_u, κ, R are damage related material constants.

The best way to determine the damage evolution parameters would be experimental techniques (such as X-ray and radiographic methods) in which the actual effects of crack propagation are measured. Since such techniques are not readily available, parameters are indirectly evaluated from the observed stress–strain relations. An algorithm for evaluation of r_u, κ, R is presented in the Appendix. After these parameters (κ, R, r_u) are known, the value of r corresponding to every σ_{ij} is known, and from eqn (2), we obtain

$$\sigma^1_{ij} = \frac{\sigma_{ij}}{(1-r)} - \frac{r}{3(1-r)}\sigma_{kk}\delta_{ij}. \tag{23}$$

Thus σ^1_{ij} and ε_{ij} are known at every point in the available experiments. Since σ^1_{ij} and ε_{ij} are related through the elastoplastic eqn (3), determination of the elastoplastic parameters is straightforward; details are given in Refs [41, 42].

Table 1

Constant	Value	Units
Damage		
r_u	0.875	—
R	1.502	—
κ	668.0	—
Plasticity		
β	1.0383	—
γ	0.0678	—
n	5.24	—
α_1	4.9×10^{-6} } $\alpha_0 = 1\,\mathrm{N\,mm^{-2}}$	—
η_1	0.849	—
b	36.6	$\mathrm{N\,mm^{-2}}$
Elasticity		
E (Young's modulus)	37,000	$\mathrm{N\,mm^{-2}}$
ν (Poisson's ratio)	0.25	—

Note: no units indicates a dimensionless constant.

9. ANALYSIS AND NUMERICAL IMPLEMENTATION

The proposed models have been studied for uniqueness in the softening regime[44]. It is shown that the constitutive equations lead to a unique solution for the case of rate-dependent models as well as for rate-independent models. Subsequently the models' implementation in finite element analysis shows mesh size insensitivity in the hardening and softening regimes. Conditions for localization of deformation (so-called narrow "shear band" formation) are also developed and discussed in Ref. [44]. Further, in Ref. [27], energy considerations show the equivalence of the two fraction body to an elastic–plastic body containing cracks.

10. TEST DATA AND CONSTANTS

Laboratory test results for concrete[12] were used for determination of parameters involved in the theory, and comparison of predictions with the experimental results. The concrete used in Ref. [12] had a cement content of $320\,\mathrm{kg\,m^{-3}}$; Portland cement (Type A) was used. The water cement (w/c) ratio was 0.50, and the maximum aggregate size was 16 mm. The recorded cylindrical strength was $f'_c = 38.1\,\mathrm{N\,mm^{-2}}$.

Cubical specimens of 100 mm size were cast and tested in a truly triaxial device with stiff loading frames and servo-hydraulic actuators. Uniaxial, biaxial and triaxial tests were also performed with a loading speed between $\dot{\varepsilon} = 5 \times 10^{-6}$ and $20 \times 10^{-6}\,\mathrm{s^{-1}}$, where $\dot{\varepsilon}$ denotes strain rate. These loading speeds are considered as slow, and the effect of the range of speeds on the stress–strain behavior was not significant.

The constants for the concrete material were determined from a number of tests, and they are listed in Table 1.

11. COMPARISON WITH EXPERIMENTAL DATA

The constants shown in Table 1 were used to define the proposed model, which was used to derive incremental eqn (13). These equations were integrated along various stress paths to predict corresponding stress–strain response.

The proposed model was verified by back-predicting observed curves for different stress paths. Here only typical results for the concrete, described above, are presented. Further verification with respect to a soil and a sandstone as well as application with respect to finite element procedures are presented in Refs [11,45].

Figure 9 shows comparisons between predictions and observations for a multiaxial stress path such that $\sigma_1/\sigma_2 = \sigma_1/\sigma_3 = 10$. Figure 9(a) shows curves for major (compressive) strain, ε_1, vs τ_{oct}; τ_{oct} denotes the octahedral shear stress. In Fig. 9(b), plots of minor (tensile) strain, ε_2, vs τ_{oct} are shown, and Fig. 9(c) shows results for ε_1 vs ε_v, where ε_v denotes the

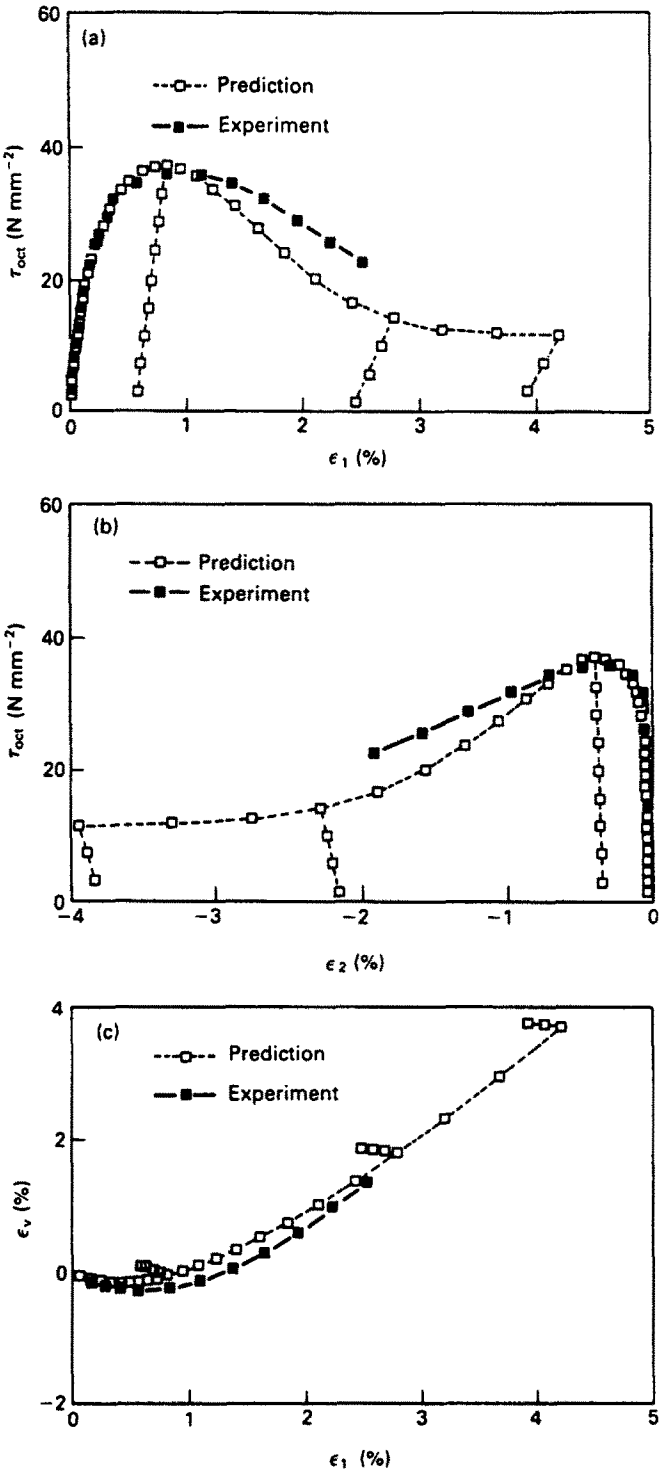

Fig. 9. Comparisons for constant stress ratio test: $\sigma_1/\sigma_2 = \sigma_1/\sigma_3 = 10$. Experimental data after Ref. [12]. (a) ε_1–τ_{oct}; (b) ε_2–τ_{oct}; (c) ε_1–ε_v.

volumetric strain. Similar results for a test with $\sigma_1/\sigma_2 = 3.33$ and $\sigma_1/\sigma_3 = 20$ are shown in Fig. 10. Comparisons between predictions and observations for a uniaxial compression test are shown in Fig. 11. Based on Figs 9–11, the following observations are made.

(1) The model predicts observed response in which the material initially compacts and then dilates. The volumetric predictions show good correlation with observed response

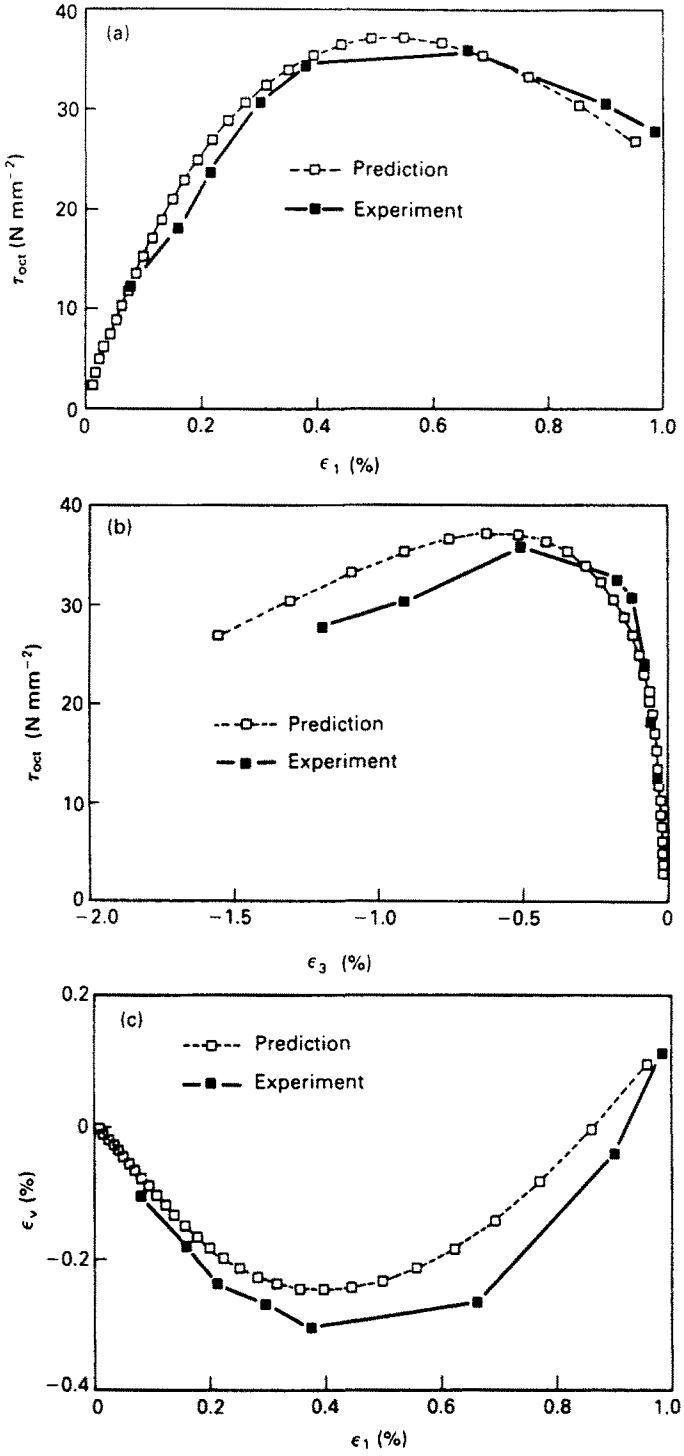

Fig. 10. Comparisons for constant stress ratio test: $\sigma_1/\sigma_2 = 3.33$, $\sigma_1/\sigma_3 = 20$. Experimental data after Ref. [12]. (a) ε_1–τ_{oct}; (b) ε_3–τ_{oct}; (c) ε_1–ε_v.

and the point of dilatation which occurs in the pre-peak region, close to the peak, is also captured.

(2) The prediction of the behavior is highly satisfactory for the major and minor strains.

Overall, the model provides very good predictions for the behavior of concrete considered herein.

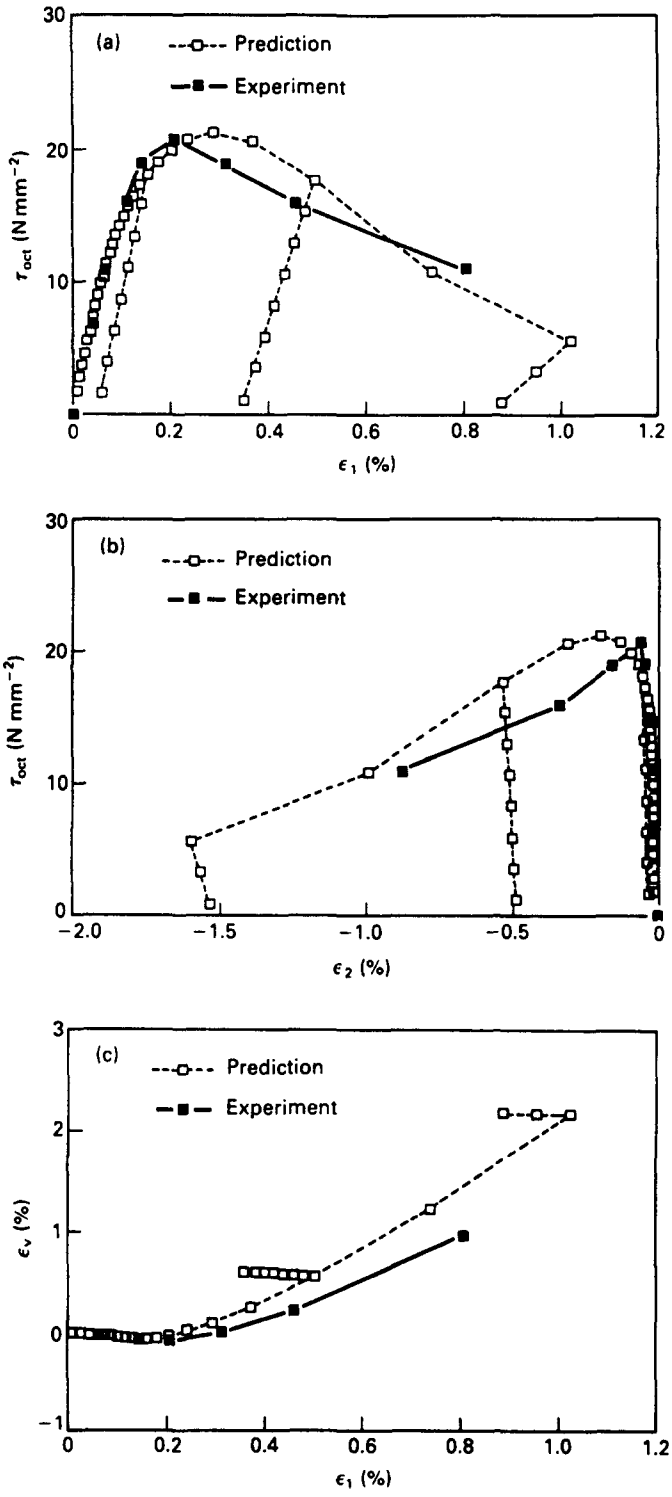

Fig. 11. Comparisons for uniaxial compression test. Experimental data after Ref. [12]. (a) ε_1–τ_{oct}; (b) ε_2–τ_{oct}; (c) ε_1–ε_v.

11.1. *Comments*

The model proposed in this paper is based on phenomenological considerations and accounts for change (loss) of strength and induced anisotropy due to microcracking and fracturing; it is not intended for detailed identification of location and directional propagation of cracks.

In the present formulation, the topical part was assumed elastoplastic; thus, only a

part of the material follows plasticity while the overall model allows for effects that may not be dependent on plastic flow. Also, the model can permit introduction of any appropriate constitutive description to simulate the topical part for a given material.

The model considers unloading and reloading to be linearly elastic; it is possible, however, to include a hysteresis loop by extending the plasticity model for unloading and reloading, with further accumulation of damage.

At this time, the present formulation is developed and applied with respect to test data from one size of specimens. It is noted that softening response is dependent on the size and shape of specimens [2, 12]. The proposed model can be extended to allow for these effects with an appropriate theory such as the non-local concept, and relevant laboratory tests.

12. CONCLUSIONS

A constitutive model based on the idea of damage is developed and applied for strain-softening behavior. Strain softening is not treated as a continuum material property, but a result of nonhomogeneity in the deformation and stress fields. It is shown that damage evolution is responsible for the observed degradation of strength and (unloading) shear modulus, as well as induced anisotropy. The model is relatively simple and identification and calibration of material constants is straightforward. The model provides satisfactory predictions of the observed response, although it is simple, and is by no means complete. Extension to tensile stress conditions, anisotropic and inelastic unloading and reloading, and response under sequential loading are some of the subjects that need further investigation. Also, the proposed theory should be tested with respect to specially designed experiments; e.g. one such procedure would be identification of the measure of induced anisotropy through experiments, and then back prediction of this measure through the anisotropy involved in the model [eqn (13)].

Acknowledgments—The results presented in this paper were obtained under a research grant No. CEE-8215344 by the National Science Foundation, Washington, D.C., and Grant No. AFOSR-83-0256 from Air Force Office of Scientific Research (AFOSR).

REFERENCES

1. I. S. Sandler, Strain softening for static and dynamic problems. ASME Winter Annual Meeting, Symp. on Constitutive Equations: Micro, Macro and Computational Aspects, CEQ, New Orleans (December 1984).
2. H. E. Read and G. A. Hegemier, Strain softening of rock, soil and concrete—a review article. *Mech. Mater.* **3**, 271–294 (1984).
3. K. C. Valanis, On the uniqueness of solution of the initial value problem in softening materials. *J. Appl. Mech. ASME* **52**, 85-APM-29 (1985).
4. S. T. Pietruszczak and Z. Mroz, Finite element analysis of deformation of strain-softening materials. *Int. J. Numer. Meth. Engng* **17**, 327–334 (1981).
5. F. H. Wu and L. B. Freund, Deformation trapping due to thermoplastic instability in one-dimensional wave propagation. *J. Mech. Phys. Solids* **32**, 119–132 (1984).
6. J. A. Hudson, E. T. Brown and C. Fairhurst, Shape of the complete stress–strain curve for rock. *Proc. 13th Symp. Rock Mech.*, University of Illinois, Urbana, Illinois (1971).
7. D. K. Hallbauer, H. Wagner and N. G. W. Cook, Some observations concerning the microscopic and mechanical behavior of quartzite specimens in stiff, triaxial compression tests. *Int. J. Rock Mech. Min. Sci.* **10**, 713–718 (1973).
8. B. T. Brady, W. I. Duvall and F. G. Horimo, An experimental determination of the true uniaxial stress–strain behavior of brittle rock. *Rock Mech.* **5**, 107–120 (1973).
9. A. Hettler and I. Vardoulakis, Behavior of dry sand tested with a large triaxial apparatus. *Géotechnique* **34**, 183–198 (1984).
10. S. P. Shah and F. O. Slate, Internal microcracking, mortar–aggregate bond and the stress–strain curve of concrete. *Proc. Int. Conf. on the Structure of Concrete and its Behavior Under Load*, London (Sept. 1965).
11. G. Frantziskonis, Progressive damage and constitutive behavior of geomaterials including analysis and implementation. Ph.D. dissertation, Dept. of Civil Engng and Engng Mech., University of Arizona, Tucson, Arizona (1986).
12. J. G. M. Van Mier, Strain softening of concrete under multiaxial loading conditions. Doctoral dissertation, Eindhoven University of Technology, The Netherlands (1984).
13. L. M. Kachanov, *The Theory of Creep* (Edited by A. J. Kennedy), Chaps IX and X. National Lending Library, Boston (1958), English translation.
14. Y. N. Rabotnov, *Creep Problems in Structural Members*. North-Holland, Amsterdam (1969).

15. D. C. Drucker, Some classes of inelastic materials, related problems basic to future technologies. *Nucl. Engng Des.* **57**, 309–322 (1980).
16. C. S. Desai, A consistent finite element technique for work-softening behavior. *Proc. Int. Conf. on Comp. Methods in Nonlinear Mechanics* (Edited by J. T. Oden *et al.*), University of Texas, Austin, Texas (1974).
17. D. R. Hayhurst and F. A. Leckie, The effect of creep constitutive and damage relationships upon the rupture time of a solid circular torsion bar. *J. Mech. Phys. Solids* **21**, 431–446 (1973).
18. D. R. Hayhurst, P. R. Dimer and M. W. Chernuka, Estimates of the creep rupture lifetime of structures using the finite element method. *J. Mech. Phys. Solids* **23**, 335–355 (1975).
19. K. E. Loland, Continuous damage model for load response estimation of concrete. *Cement Concrete Res.* **10**, 395–402 (1980).
20. J. Mazars, Mechanical damage and fracture of concrete structures. Advances in Fracture Research, 5th Int. Conf. Fracture, Cannes, Vol. 4, pp. 1499–1506 (1981).
21. J. W. Dougill, On stable progressively fracturing solids. *Z. Angew. Math. Phys.* **27**(4), 423–437 (1976).
22. J. W. Dougill and M. A. M. Rida, Further consideration of progressively fracturing solids. *J. Engng Mech. Div. ASCE* **106**, 1021–1038 (1980).
23. Z. P. Bazant and S. S. Kim, Plastic fracturing theory for concrete. *J. Engng Mech. Div. ASCE* **105**, 407–478 (1979).
24. D. R. Curran, L. Seaman and J. Dein, *Constitutive Laws for Failing Materials, Mechanics of Engineering Materials* (Edited by C. S. Desai and R. H. Gallagher), pp. 139–152. Wiley, Chichester (1984).
25. L. Davison and A. L. Stevens, Thermomechanical constitution of spalling elastic bodies. *J. Appl. Phys.* **44**, 668–673 (1973).
26. A. Drescher and I. Vardoulakis, Geometric softening in triaxial tests on granular material. *Géotechnique* **32**, 291–303 (1982).
27. G. Frantziskonis and C. S. Desai, Elastoplastic model with damage for strain softening geomaterials. *Acta Mech.* (1987), in press.
28. R. Hill, *The Mathematical Theory of Plasticity*. Oxford University Press, Oxford (1950).
29. T. C. Hsu, F. D. Slate, G. M. Sturman and G. Winter, Microcracking of plain concrete and the shape of the stress–strain curve. *J. Am. Concr. Inst.* **60**, 227–239 (1963).
30. D. C. Spooner and J. W. Dougill, A quantitative assessment of damage sustained in concrete during compressive loading. *Mag. Concr. Res.* **27**, 151–160 (1975).
31. W. R. Wawersik and C. Fairhurst, A study of brittle rock fracture in laboratory compression experiments. *Int. J. Rock Mech. Min. Sci.* **7**, 561–575 (1970).
32. T. Hueckel, On plastic flow granular and rock like materials with variable elasticity moduli. *Bull. Pol. Acad. Sci. Sec. Sci. Tech.* **23**, 405–414 (1975).
33. G. Maier, Nonassociated and coupled flow rules of elastoplasticity for geotechnical media. *Proc. Int. Conf. on Soil Mech. and Found. Engng*, Tokyo (1977).
34. Y. F. Dafalias, Modeling cyclic plasticity: simplicity versus sophistication. In *Mechanics of Engineering Materials* (Edited by C. S. Desai and R. H. Gallagher), pp. 153–178. Wiley, Chichester (1984).
35. B.-L. Young, Y. F. Dafalias and L. R. Herrmann, A bounding surface plasticity model for concrete. *J. Engng Mech. Div. ASCE* **111**, 359–380 (1985).
36. C. S. Desai, A general basis for yield, failure and potential functions in plasticity. *Int. J. Numer. Analyt. Meth. Geomech.* **4**, 361–375 (1980).
37. C. S. Desai and H. J. Siriwardane, *Constitutive Laws for Engineering Materials*. Prentice-Hall, Englewood Cliffs, New Jersey (1983).
38. R. Baker and C. S. Desai, Induced anisotropy during plastic straining. *Int. J. Numer. Analyt. Meth. Geomech.* **8**, 167–185 (1984).
39. C. S. Desai and M. O. Faruque, Constitutive model for (geological) materials. *J. Engng Mech. Div. ASCE* **110**, 1391–1408 (1984).
40. M. O. Faruque and C. S. Desai, Implementation of a general constitutive model for geological materials. *Int. J. Numer. Analyt. Meth. Geomech.* **9** (1985).
41. C. S. Desai, S. Somasundaram and G. Frantziskonis, A hierarchical approach for geologic materials. *Int. J. Numer. Analyt. Meth. Geomech.* **10** (1986).
42. G. Frantziskonis, C. S. Desai and S. Somasundaram, Constitutive model for nonassociative behavior. *J. Engng Mech. Div. ASCE* **112**, 932–946 (1986).
43. M. R. Salami, Constitutive modelling of concrete and rocks under multi-axial compressive loading. Ph.D. dissertation, University of Arizona, Tucson, Arizona (1986).
44. G. Frantziskonis and C. S. Desai, Analysis of strain softening constitutive model. *Int. J. Solids Structures* **23**, 751–767 (1987).
45. C. S. Desai and G. Frantziskonis, A strain-softening model and application to soil and rock behavior (1987); to be published.

APPENDIX

Topical response parameters are found from the available test data. Parameters β, γ are determined from ultimate stress states of different tests, hardening parameters α_1, η_1 from the stress–strain response, and the elasticity parameters E, ν from available unloading–reloading stress–strain curves. Further details are given in Refs [41, 42].

Parameter r_u is determined from shear tests, and it is directly related to the ratio of $\sqrt{J_{2D}}$ at the residual stress level divided by the value of $\sqrt{J_{2D}}$ at the peak. Given a stress–strain curve (curve (a) in Fig. 4) at the residual stress level, we have $(1 - r_u) = (\sqrt{J_{2D}})_{res}/(\sqrt{J_{2D}})_{ult}$ where the subscript "res" indicates residual stress level and "ult" indicates ultimate conditions. The ultimate condition is close to the peak and represents the asymptotic value to the prepeak curve. Thus

$$r_u \cong 1 - (\sqrt{J_{2D}})_{res}/(\sqrt{J_{2D}})_{peak}. \tag{A1}$$

This relation is used to find the value of r_u. After r_u is known, κ and R are determined from back-analysis of eqn (22) through a least square fit on a number of points on the stress–strain curve. The value of r at each point is given by

$$r \cong 1 - (\sqrt{J_{2D}})/(\sqrt{J_{2D}})_{peak} \tag{A2}$$

where $\sqrt{J_{2D}}$ corresponds to a given point.